

# Electrical Characterisation of electron beam exposure induced Defects in silicon



Helga T. Danga\*, Francois D. Auret, Sergio M.M. Coelho, Mmantsae Diale

Department of Physics, University of Pretoria, Pretoria 0002

## ARTICLE INFO

### Article history:

Received 15 May 2015

Received in revised form

22 July 2015

Accepted 23 July 2015

Available online 26 July 2015

### Keywords:

Silicon

Electron beam exposure

DLTS

Laplace-DLTS

## ABSTRACT

The defects introduced in epitaxially grown p-type silicon (Si) during electron beam exposure were electrically characterised using deep level transient spectroscopy (DLTS) and high resolution Laplace-DLTS. In this process, Si samples were first exposed to the conditions of electron beam deposition (EBD) without metal deposition. This is called **electron beam exposure (EBE)** herein. After 50 minutes of EBE, nickel (Ni) Schottky contacts were fabricated using the resistive deposition method. The defect level observed using the Ni contacts had an activation energy of H(0.55). This defect has an activation energy similar to that of the I-defect. The defect level is similar to that of the HB4, a boron related defect. DLTS depth profiling revealed that H(0.55) could be detected up to a depth of 0.8  $\mu\text{m}$  below the junction. We found that exposing the samples to EBD conditions without metal deposition introduced a defect which was not introduced by the EBD method. We also observed that the damage caused by EBE extended deeper into the material compared to that caused by EBD.

© 2015 Elsevier B.V. All rights reserved.

## 1. Introduction

Electron beam deposition (EBD) of metals in a vacuum system plays an important role in the semiconductor technology industry. This method is useful when it comes to depositing materials with a high melting point which cannot be evaporated by resistive heating because of limitations of the power input [1]. The disadvantage of EBD is that this technique introduces defects in n-type Si close to the metal-silicon interface [2]. These defects influence device performance and alter the barrier heights of the contacts [3]. The defects responsible for these barrier modifications are formed when energetic particles reach the semiconductor surface and interact with it, resulting in lattice damage. Depending on the application, these defects may either be beneficial or detrimental for optimum device functioning. In silicon, for example, defect introduction during high energy electron and proton irradiation increases the switching speed of devices [4]. On the other hand, in the case of high open circuit voltage solar cells, degraded device properties have been reported after EBD of contacts [5,6].

The main aim of developing the EBE technique was to see if EBD induced defects could be introduced in a controlled manner. Excessive exposure would reduce the functionality of diodes for further study thus putting a limit on how much damage could be introduced. Energetic particles that cause EBD damage are present

during EBE but interact directly with the semiconductor material whereas during EBD this interaction mostly occurs via the metal used as a contact [7]. Silicon (Si) is one of the most important semiconductor materials and it has been studied extensively [8]. This is mainly due to its low cost, thermal stability, and good durability [9]. It is because of these properties that Si is a suitable candidate for exploring the EBE technique.

In this paper we report the defects introduced in epitaxially grown, boron-doped, p-type Si. In addition, we identify the  $C_i$  and the I-defect. We demonstrate that when exposing the sample to EBD conditions without depositing any metal, different defects are introduced.

## 2. Experimental Details

Epitaxially grown boron-doped p-type Si  $\langle 111 \rangle$  grown on  $p^+$  Si substrate was investigated. Before metallisation the samples were first degreased and then dipped in hydrofluoric acid (HF) for 1 minute to etch off the native oxide layer. Directly after cleaning the samples were inserted into the vacuum system. Vacuum pumping was carried out by a dry pump in series with a turbo molecular pump to lower the  $H_2$  concentration. To improve the vacuum, titanium (Ti) was deposited in the chamber with the sample rotated away from the evaporation source. While the pre-deposition vacuum was typically  $5 \times 10^{-7}$  mbar, this soon increased to approximately  $3 \times 10^{-6}$  mbar during the evaporation. As the vacuum conditions vary greatly during EBD, forming gas

\* Corresponding author.

E-mail address: [helga.danga@up.ac.za](mailto:helga.danga@up.ac.za) (H.T. Danga).

H15, with a composition of  $N_2:H_2$  of 85%: 15% by volume was also used to raise the pressure in the vacuum chamber to  $10^{-4}$  mbar and kept constant during processing of samples selected for EBE. Electron beam exposure of samples and the fabrication of contacts using electron beam deposition were done by utilising a 10 kV source (MDC model e-Vap 10CVS) with the samples positioned 50 cm above the crucible [5].

During EBE, without metal deposition, the samples were exposed for 50 minutes; while the beam heated a tungsten source using a beam current of 100 mA, this current being insufficient to evaporate tungsten, thus exposing the samples to EB conditions comparable to those experienced during deposition. Ni diodes were used for all the samples prepared for this study as this metal can be evaporated resistively, a process that is known to not introduce defects in concentrations measurable by deep level transient spectroscopy (DLTS) [5]. A control sample was prepared by resistively depositing aluminium (Al) contacts onto p-type epitaxial material without using EB exposure. A sample with Al contacts irradiated with alpha-particles at a fluence of  $5.1 \times 10^{10} \text{ cm}^{-2}$  was also used in this study for comparison. DLTS and high resolution Laplace-DLTS were used to characterise the defects introduced in epitaxially grown p-type Si during EBE and EBD

### 3. Results and discussion

In this study, the following defects were observed: (H0.59), H(0.55), H(0.52), H(0.33) and H(0.16). The defect level observed using the Nickel contacts after EBE (spectrum (c) in Fig.1) had an activation energy of H(0.55) with an apparent capture cross-section of  $6.6 \times 10^{-14} \text{ cm}^2$ . This defect had an activation energy similar to the I-defect. Pintilie et al. [10] observed a defect with a similar energy of 0.545 eV with an apparent capture cross-section of  $9.0 \times 10^{-14} \text{ cm}^2$ . This defect was observed after exposing their samples to high irradiation fluences. The defect level was detected using thermally stimulated current (TSC). The H(0.55) defect is aligned to the defect H(0.52) as shown in Fig.2. This defect was introduced by alpha-particle irradiation. It had an apparent capture cross-section of  $1.7 \times 10^{-14} \text{ cm}^2$  and its temperature peak was at 246 °C. Nyamhere et al. measured a defect they referred to as HB4, a defect having an apparent cross-section of  $1.3 \times 10^{-13} \text{ cm}^2$ . It had an activation enthalpy of 0.54 eV and its peak temperature

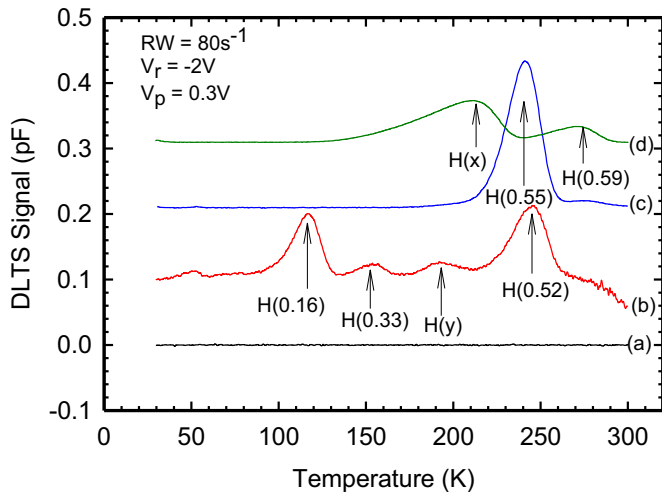


**Fig. 1.** DLTS spectra for (a) a control spectrum measured from Al Schottky diodes fabricated using resistive deposition, (b)  $\alpha$ -particle irradiated Al Schottky diodes, (c) Ni Schottky diodes fabricated after EBE and (d) Ni Schottky diodes fabricated using the EBD method.

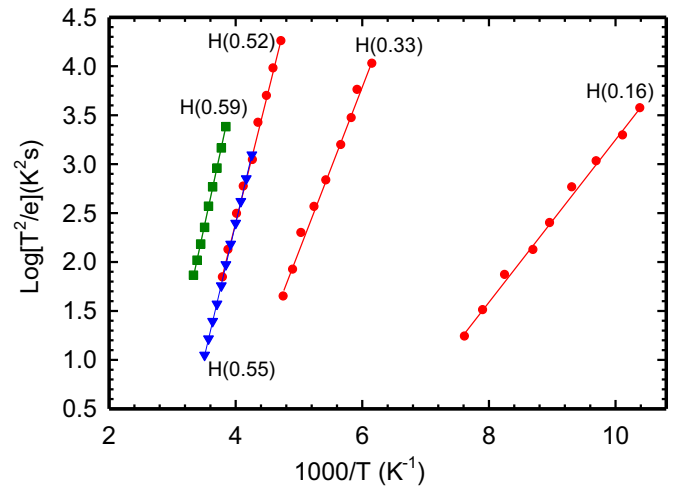


**Fig. 2.** Arrhenius plots for defects introduced after: samples exposed to electron beam conditions (EBE) thereafter Ni Schottky diodes fabricated (down triangles);  $\alpha$ -particle irradiated Al Schottky diodes (circles) and Ni Schottky contacts fabricated using the EBD method (squares).

was at 240 °C. This peak temperature was similar to that of H(0.55), which lay at 242 °C. HB4 was attributed to interstitial boron-substitutional boron-hydrogen ( $B_i-B_s-H$ ) complex [11–14].

For Ni contacts fabricated using EBD, spectrum (d) in Fig.1, we observed the defect level H(0.59). This defect had a similar activation enthalpy and apparent capture cross-section as that of HB5, a defect observed by Nyamhere et al. [14]. In their study of EBD processed induced defects and their annealing behaviour, it was proposed that the breakup of the 0.54 eV defect level was responsible for the introduction of the 0.59 eV level. This defect was boron related [14]. We were unable to resolve the peak H(x) using  $\iota$ -DLTS. This peak could have been a surface state or an extension of a defect.

From the spectrum shown in Fig.1(b), for the alpha-particle irradiated Al contacts, the hole traps observed were: H(0.16), H(0.33) and H(0.52). The defect level H(0.33) was identified as the interstitial carbon ( $C_i$ ) related defect. It was a result of induced damage and could only be explained by the presence of donor-like traps [7]. The capture cross-section was calculated to be  $1.6 \times 10^{-19} \text{ cm}^2$  from the Arrhenius plot shown in Fig. 2. Auret et al. observed a defect in p-type silicon with the same activation energy in samples that had been fabricated with titanium contacts using the resistive deposition method [15]. Defects with a similar activation energy (H(0.33)) have been identified in the literature. These are all related to the residual carbon impurity which has been reported to form complexes directly with radiation-produced primary defects or with secondary defects induced by radiation damage. These defects include the interstitial-carbon-interstitial-oxygen ( $C_i - O_i$ ) complex (C(3) centre) [16], the carbon-oxygen-vacancy complex (the K centre) [17,18] and the interstitial-substitutional-carbon complex ( $C_s - C_i$ ) [19–21]. In their study, Asghar et al. observe that the 0.35 eV defect annealed at approximately 400 °C in agreement with the literature of similar defect levels  $E_v + 0.38$  and  $E_v + 0.33$  [17,18]. These reports suggest that this level originates from the carbon-oxygen-vacancy ( $C - O - V$ ) complex. However, studies by Song et al. [22] strongly suggest this defect to be associated with  $C_i - O_i$  complex. This deep level would be expected to be strongly dependant on the material and sample since unintentional carbon and oxygen contamination could vary with the material growth technique used as well as device processing. It seems that H(0.52) is a boron impurity related defect. This defect was attributed to EBD damage. [14]. The identity of H(0.16) has not been established. Resolving the identity of peak H(y) using  $\iota$ -DLTS

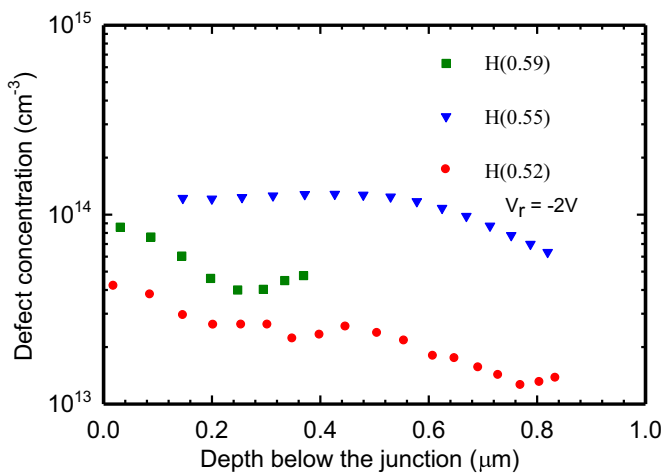


Fig. 3. Depth concentration profiles of H(0.59) a defects introduced by EBD, H(0.55) is a defect introduced during EBE and H(0.52) is a defect level introduced by  $\alpha$ -particle irradiation.

proved to be a challenge. It may have been an extension of a neighbouring defect.

The aim of depth profiling was to find the defect concentration as a function of depth for individual defects. Fixed bias-variable pulse Laplace-DLTS depth profiling [6,23] was used to measure the depth distribution of the defects investigated in this study. For each defect, the temperature was kept constant, the reverse bias of  $-2$  V was maintained while varying the filling pulse. Fig. 3 illustrates the results obtained. Depth profiling of the defects showed that as we probed deeper into the bulk away from the junction, the H(0.55) defect decreased from  $1 \times 10^{14} \text{ cm}^{-3}$  at the metal-semiconductor interface to  $6 \times 10^{13} \text{ cm}^{-3}$  about  $0.8 \mu\text{m}$  below the interface. The defect level H(0.59) introduced by EBD, decreased from  $2 \times 10^{14} \text{ cm}^{-3}$  at the interface to about  $5 \times 10^{13} \text{ cm}^{-3}$  at  $0.4 \mu\text{m}$  below the junction. In the case of the defect level H(0.52), the defect concentration showed a decrease from  $4 \times 10^{13} \text{ cm}^{-3}$  at the junction to  $1 \times 10^{13} \text{ cm}^{-3}$  at approximately  $0.8 \mu\text{m}$  below the junction. This implies that the damage caused by EBE extends deeper into the material when compared to EBD. This is because during EBD, the metal deposited shields the semiconductor material from the energetic particles which would otherwise have more energy when interacting with the material.

#### 4. Conclusion

We observed that the EBE process induced a different defect to the one observed in the EBD. H(0.55) for Ni contacts was associated with the I-centre. The defect H(0.59) was observed after EBD. H(0.59) was a boron related defect. The hole traps observed for alpha-particle irradiated Al contacts were: H(0.16), H(0.33) and

H(0.52). H(0.33) was identified as the interstitial carbon ( $C_i$ ) related defect and H(0.52) was identified as a boron impurity related defect. This study revealed that a different defect is introduced during EBE which is not introduced by EBD method. The H(0.55) defect level seems to have been of the same origin as H(0.52), a defect introduced by alpha-particle irradiation. Laplace-DLTS depth profiling revealed that H(0.55) could be detected up to a depth of  $0.8 \mu\text{m}$ . The EBD defect observed was at  $0.4 \mu\text{m}$  below the junction. The defect introduced by alpha-particle irradiation extended to a depth of about  $0.83 \mu\text{m}$ . The damage caused by EBE extends deeper into the material compared to EBD but not as deep as alpha-particles. This was attributed to the shielding effect the deposited metal has on the semiconductor material from the energetic particles which would otherwise extend deeper into the material.

#### Acknowledgements

The authors would like to thank the National Research Foundation of South Africa for the financial support. We also thank Mr P.J. Janse van Rensburg for his technical assistance.

#### References

- [1] F.D. Aurret, P.M. Mooney, American Institute of Physics 55 (1983).
- [2] F.D. Aurret, P.M. Mooney, J. Appl. Phys. 55 (1984).
- [3] G. Myburg, F.D. Aurret, J. Appl. Phys. 71 (1992).
- [4] D.C. Swako, J. Bartko, IEEE Nucl. Sci. 30 (1983).
- [5] A.W. Blakers, M.A. Green, IEEE Electron Device Letters (1984) 246.
- [6] F.D. Aurret, S.M.M. Coelho, J. Nel, W.E. Meyer, Phys. Status Solidi A 209 (2012) 1926–1933.
- [7] O. Paz, F.D. Aurret, Mat. Res. Soc. Symp. 25 (1984).
- [8] S.M. Sze, Physics of Semiconductor Devices, Second ed., John Wiley and Sons (WIE), 1981.
- [9] (<http://www.americanphotonics.com/si.php>), 2009.
- [10] I. Pintilie, M. Buda, E. Fretwurst, G. Lindstrom, J. Stahl, Nuclear Instruments and Methods in Physics Research A 556 (2006) 197–208.
- [11] O. Feklisova, N. Yarikin, E.B. Yakimov, J. Weber, Physica B (2001) 210–212.
- [12] M. Mamor, M. Willander, F.D. Aurret, W. Meyer, E. Sveinbjornsson, Phys. Rev. B 63 (2000).
- [13] F. Volpi, A.R. Peaker, I. Berebezier, A. Ronda, J. Appl. Phys. 95 (2004).
- [14] C. Nyamhere, A.G.M. Das, F.D. Aurret, M.H. C., Journal of Physics Conference Series, IOP, 2008.
- [15] F.D. Aurret, R. Kleinhenz, C.P. Schnider, Appl. Phys. Lett. 44 (1984).
- [16] J.M. Trombetta, G.D. Watkins, Appl. Phys. Lett. 51 (1987).
- [17] P.M. Mooney, L.J. Cheng, M. Sulli, J.D. Gerson, J.W. Corbett, Phys. Rev. B 15 (1977).
- [18] Y.H. Lee, K.L. Wang, A. Jaworowski, P.M. Mooney, L.J. Cheng, J.W. Corbett, Phys. Status Solidi A 57 (1980) 697.
- [19] L.C. Kimberling, International Conference On Radiation Effects On Semiconductors, in: N.B. Urli, J.W. Corbett (Eds.), Inst. Phys., Bristol, 1977, p. 221, Ser.No.
- [20] L.C. Kimberling, IEEE Trans. Nucl. Sci. NS-23 (1976) 1497.
- [21] M. Asghar, M.Z. Iqbal, N. Zafar, American Institute of Physics 73 (1993).
- [22] L.W. Song, X.D. Zhan, B.W. Benson, G.D. Watkins, Physical Review B 42 (1990).
- [23] Y. Zohta, M.O. Watanabe, J. Appl. Phys. 53 (1982).